PNAS RESEARCH ARTICLE | NEUROSCIENCE OPEN ACCESS

Activity-dependent endoplasmic reticulum Ca^{2+} uptake depends on Kv2.1-mediated endoplasmic reticulum/plasma membrane junctions to promote synaptic transmission

Lauren C. Panzera[a], Ben Johnson[b], Josiah A. Quinn[b], In Ha Cho[a], Michael M. Tamkun[b], and Michael B. Hoppa[a,1]

Edited by Pietro De Camilli, Yale University, New Haven, CT; received September 17, 2021; accepted June 15, 2022

The endoplasmic reticulum (ER) forms a continuous and dynamic network throughout a neuron, extending from dendrites to axon terminals, and axonal ER dysfunction is implicated in several neurological disorders. In addition, tight junctions between the ER and plasma membrane (PM) are formed by several molecules including Kv2 channels, but the cellular functions of many ER-PM junctions remain unknown. Recently, dynamic Ca^{2+} uptake into the ER during electrical activity was shown to play an essential role in synaptic transmission. Our experiments demonstrate that Kv2.1 channels are necessary for enabling ER Ca^{2+} uptake during electrical activity, as knockdown (KD) of Kv2.1 rendered both the somatic and axonal ER unable to accumulate Ca^{2+} during electrical stimulation. Moreover, our experiments demonstrate that the loss of Kv2.1 in the axon impairs synaptic vesicle fusion during stimulation via a mechanism unrelated to voltage. Thus, our data demonstrate that a nonconducting role of Kv2.1 exists through its binding to the ER protein VAMP-associated protein (VAP), which couples ER Ca^{2+} uptake with electrical activity. Our results further suggest that Kv2.1 has a critical function in neuronal cell biology for Ca^{2+} handling independent of voltage and reveals a critical pathway for maintaining ER lumen Ca^{2+} levels and efficient neurotransmitter release. Taken together, these findings reveal an essential nonclassical role for both Kv2.1 and the ER-PM junctions in synaptic transmission.

endoplasmic reticulum | synaptic transmission | calcium | exocytosis | Kv2

Significance

The endoplasmic reticulum (ER) extends throughout the neuron as a continuous organelle, and its dysfunction is associated with several neurological disorders. During electrical activity, the ER takes up Ca^{2+} from the cytosol, which has been shown to support synaptic transmission. This close choreography of ER Ca^{2+} uptake with electrical activity suggests functional coupling of the ER to sources of voltage-gated Ca^{2+} entry through an unknown mechanism. We report that a nonconducting role for Kv2.1 through its ER binding domain is necessary for ER Ca^{2+} uptake during neuronal activity. Loss of Kv2.1 profoundly disables neurotransmitter release without altering presynaptic voltage. This suggests that Kv2.1-mediated signaling hubs play an important neurobiological role in Ca^{2+} handling and synaptic transmission independent of ion conduction.

The members of the Kv2 family of voltage-gated K^+ (Kv) channels, Kv2.1 and Kv2.2, are widely expressed in neurons within the mammalian brain, with Kv2.1 dominating in hippocampal neurons (1–3). These channels play an important classical role in repolarizing somatic membrane potential during high-frequency stimulation (4). However, Kv2 channels also form micrometer-sized clusters on the cell membrane, where they are largely nonconductive (5). When clustered, these nonconductive channels act as molecular hubs directing protein insertion and localization, including during the fusion of dense-core vesicles (6–9). Clusters are also sites for the enrichment of voltage-gated Ca^{2+} channels (10). The Kv2 clustering mechanism is due to the formation of stable tethers between the cortical endoplasmic reticulum (ER) and the plasma membrane (PM) through a noncanonical FFAT motif located on the Kv2 C terminus, which interacts with VAMP-associated protein (VAP) embedded in the ER membrane (11). These Kv2.1-mediated junctions between the ER and PM are in close (~15 nm) proximity (12), forming critical Ca^{2+}-signaling domains that have been conserved from yeast to mammals (12–14) and are necessary to cluster Kv2.1 channels. ER-PM junctions are formed by many types of proteins, although most are ER proteins that transiently interact with specific lipids on the PM (reviewed previously in ref. 15). The purpose of the Kv2.1-VAP–mediated ER-PM junction is not functionally understood in neurons to date.

Cytosolic Ca^{2+} is essential for initiating multiple cell functions, including secretion, muscle contraction, proliferation, apoptosis, and gene expression (reviewed previously in ref. 16). However, Ca^{2+} is also strongly buffered, especially in most neurons, and often requires local Ca^{2+} exchange between channels and pumps localized to organelles and the PM. The ER plays a central role in both Ca^{2+} signaling and storage (17), and dysfunction of ER morphology and Ca^{2+} handling has been linked to several unique neurological pathologies, including hereditary spastic paraplegia (18), Alzheimer's disease (19), and amyotrophic lateral sclerosis (20). Currently, the only known cellular mechanism used to replenish ER Ca^{2+} stores is through activation of store-operated Ca^{2+} entry (SOCE). Depletion of the ER's luminal Ca^{2+} is sensed by stromal interaction molecule 1 (STIM1), which aggregates and concentrates Orai proteins on the PM to initiate Ca^{2+} influx through Ca^{2+} release–activated Ca^{2+} (CRAC) channels. Recent

Author affiliations: [a]Department of Biology, Dartmouth College, Hanover, NH 03755; and [b]Department of Biomedical Sciences, Colorado State University, Fort Collins, CO 80523

Author contributions: L.C.P., M.M.T., and M.B.H. designed research; L.C.P., B.J., J.A.Q., I.H.C., M.M.T., and M.B.H. performed research; L.C.P., B.J., J.A.Q., I.H.C., M.M.T., and M.B.H. analyzed data; and L.C.P., M.M.T., and M.B.H. wrote the paper.

The authors declare no competing interest.

This article is a PNAS Direct Submission.

[1]To whom correspondence may be addressed. Email: michael.b.hoppa@dartmouth.edu.

This article contains supporting information online at http://www.pnas.org/lookup/suppl/doi:10.1073/pnas.2117135119/-/DCSupplemental.

Published July 21, 2022.

studies, however, have revealed that a second frequently accessed pathway exists in neurons where stimulation-evoked Ca^{2+} influx is rapidly taken up by the ER through sarco/endoplasmic reticulum Ca^{2+}-ATPase (SERCA) pumps during neuronal activity, rather than in reaction to severe depletion of ER lumen Ca^{2+}. Failure to quickly increase luminal Ca^{2+} during action potential (AP) firing leads to ER Ca^{2+} depletion and impaired synaptic vesicle fusion (21). Thus, luminal ER Ca^{2+} plays an essential role in maintaining synaptic transmission in active healthy neurons, suggesting that a mechanism other than SOCE must be important for neuronal communication.

Taken together, Kv2.1 clusters have been shown to localize L-type voltage-gated Ca^{2+} channels at the PM while also anchoring the ER in close proximity to the PM (10). We hypothesized that these Kv2.1-mediated ER-PM junctions are uniquely positioned to serve a critical role as dynamic signaling domains for rapid ER Ca^{2+} uptake during electrical activity in neurons. We measured Kv2.1's role in ER Ca^{2+} handling using ER-GCaMP (a genetically encoded calcium indicator) and found that AP-evoked Ca^{2+} entry into the somatic ER was absent with short hairpin RNA (shRNA) knockdown (KD) of Kv2.1 channels. This nonconducting role of Kv2.1 which enables ER-Ca^{2+} filling also requires SERCA pumps. Moreover, we demonstrate a nonconducting role for Kv2.1 in the axon that is essential for enabling ER-Ca^{2+} uptake during electrical activity. We go on to show that KD of Kv2.1 impaired overall synaptic physiology through decreased presynaptic Ca^{2+} entry and synaptic vesicle exocytosis. Finally, we demonstrate that this role requires Kv2.1's C-terminal VAP-binding domain to restore synaptic transmission.

Results

Kv2.1 Channels Have Both Conducting and Nonconducting Roles in the Soma. Kv2.1 channels are widely expressed in excitatory and inhibitory neurons in both the hippocampus (22–25) and cortex (25–28), where they have two prominent functions: 1) a conducting role repolarizing somatic membrane potential during AP firing (3, 4) and 2) a scaffolding role forming ER-PM junctions with the ER-resident protein VAP (11). We sought to quantitatively address Kv2.1 function in both roles. To measure a role in somatic AP repolarization, we first used a combination of shRNA targeting the endogenous Kv2.1 channel and the optical voltage indicator QuasAr (29, 30) in cultured hippocampal neurons. KD of Kv2.1 by shRNA resulted in a 76% reduction in immunostained Kv2.1 fluorescence intensity (*SI Appendix*, Fig. S1*A* and *B*). We also expressed the shRNA using adeno-associated virus (AAV) for high efficiency transduction and found an 80% reduction in Kv2.1 protein expression (*SI Appendix*, Fig. S1*C*). Consistent with Kv2.1's role as a delayed rectifying potassium channel, we observed no change in the AP amplitude but a robust increase (31.58%) in the full width at half maximum (FWHM) of APs recorded in the soma of cultured hippocampal neurons lacking the Kv2.1 channel (control neurons, 1.72 ± 0.078 ms; Kv2.1 KD neurons, 2.27 ± 0.106 ms; $P < 0.001$) at high-frequency stimulation (25 Hz) (Fig. 1*A*–*C*).

While conductive Kv2.1 channels have homogenous membrane expression, endogenous and transfected Kv2.1 channels also prominently localize in micrometer-sized clusters within the somatodendritic compartments and axon initial segment both in vivo and in vitro (31–33) and have been thought to be excluded from the distal axon and presynaptic terminals (25). An example is seen in a hippocampal neuron expressing Kv2.1 tagged with mGreenLantern (34), where clustering is obvious in the soma, proximal dendrites, and axon initial segments of our cultured hippocampal neurons (Fig. 1*D*), consistent with earlier findings (25, 35, 36). It has been demonstrated that Kv2.1 localization is necessary and sufficient to induce ER-PM junctions across cell types, including Human Embryonic Kidney (HEK) cells and developing hippocampal neurons (12, 37). Further, Total Internal Reflection (TIRF) imaging in young

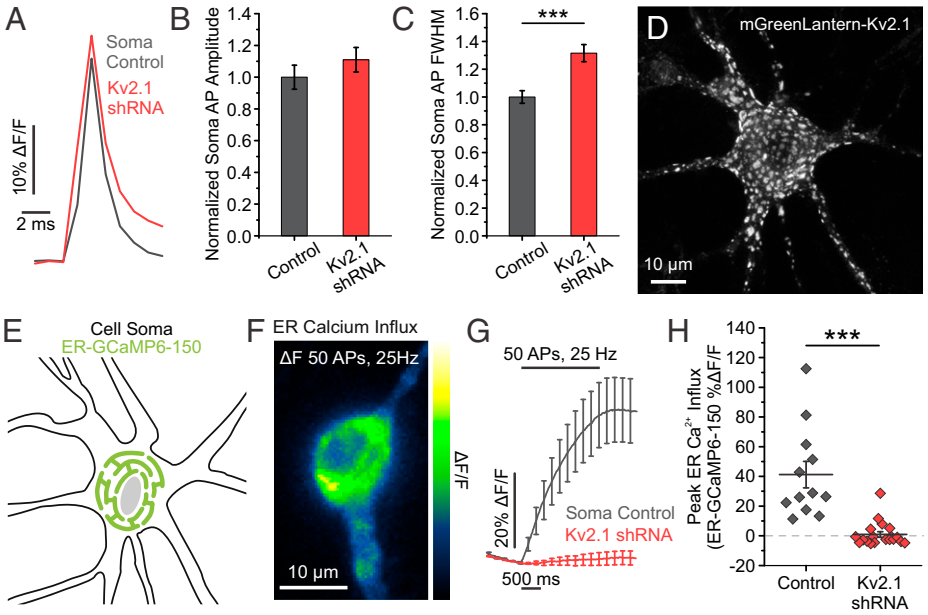

Fig. 1. Kv2.1 has both ionotropic and nonionotropic functions in the soma. (*A*) Average traces of somatic QuasAr fluorescence, trial averaged from 50 AP stimulations delivered at 25 Hz. (*B* and *C*) Quantification of AP amplitude (*B*) and FWHM (*C*) (control neurons, $n = 16$ cells; Kv2.1 KD neurons, $n = 21$ cells; ***$P < 0.001$ for FWHM comparison, Student's t test). (*D*) Example image of a cultured hippocampal neuron expressing mGreenLantern-Kv2.1. Note distinct clusters form across the membrane surface. (*E*) Cartoon of a neuronal soma expressing the fluorescent Ca^{2+} indicator ER-GCaMP6-150 in the ER lumen. (*F*) Image of the change in fluorescence of somatic ER-GCaMP6-150 in response to a train of stimulation. (*G* and *H*) Average fluorescence traces of somatic ER-GCaMP6-150 (*G*) and quantification of peak fluorescence (*H*) for both control and Kv2.1 KD neurons (control neurons, $n = 12$ cells; Kv2.1 KD neurons, $n = 19$ cells; ***$P < 0.001$, Student's t test).

cultured hippocampal neurons showed retraction of cortical ER following declustering of Kv2.1 channels (12), indicating that both the expression and placement of Kv2.1 within the membrane is important for junction formation.

Given the role of Kv2.1 clusters to both form ER-PM junctions (11) and localize voltage-gated Ca^{2+} channels (10), we were curious about the effect of interfering with Kv2.1 expression on ER Ca^{2+} uptake during electrical activity. We expressed the low-affinity ER Ca^{2+} indicator ER-GCaMP6-150 (ER-GCaMP) in cultured hippocampal neurons and measured ER Ca^{2+} influx in the soma of transfected neurons during stimulation. While a train of 50 APs normally causes a robust increase in ER Ca^{2+}, this process was severely impaired (97.64%) by KD of Kv2.1 (control neurons, 41.21 ± 8.89% ΔF/F; Kv2.1 KD neurons, 0.97 ± 1.87% ΔF/F; $P < 0.001$) (Fig. 1*G* and *H*). To ensure that this uptake was mediated by SERCA pumps, we applied the SERCA inhibitor cyclopiazonic acid (CPA), which completely blocked ER Ca^{2+} filling (control neurons before CPA, 40.85 ± 7.42% ΔF/F; and after CPA treatment, −7.74 ± 0.84% ΔF/F; $P < 0.01$) (*SI Appendix*, Fig. S2*A* and *C*). Importantly, ER Ca^{2+} influx in Kv2.1 KD neurons was impaired to the extent that SERCA inhibition had little effect during electrical activity (Kv2.1 KD neurons before CPA, 2.21 ± 3.51% ΔF/F; and after CPA treatment, −3.52 ± 1.34% ΔF/F) (*SI Appendix*, Fig. S2*B* and *C*). We also examined the effect of Kv2.1 on somatic ER Ca^{2+} refilling following store depletion with Ca^{2+}-free external solutions in developing neurons (8 d in vitro [DIV]) before significant expression of Kv2.1 channels (31, 38). TIRF imaging was used to optically isolate ER-PM junctions, and ER Ca^{2+} levels were measured with the ER-targeted fluorescent Ca^{2+} indicator CEPIA*er* (39) with and without Kv2.1 transfection as illustrated in *SI Appendix*, Fig. S3*A*. After reintroducing extracellular Ca^{2+}, the refilling rate of the cortical ER in Kv2.1-expressing neurons was fivefold greater than that observed in neurons without Kv2.1 (*SI Appendix*, Fig. S3*B*). To test whether ER-PM junction formation through VAP recruitment was sufficient to increase the rate of ER Ca^{2+} refilling, we used a chimeric approach. VAPs are typically diffusely localized in the ER, and expressing the Kv2.1 C-terminal tail including the noncanonical FFAT VAP-binding domain fused to a single-pass transmembrane glycoprotein (CD4) is sufficient to redistribute VAPs near the PM of HEK cells and neurons (11). The refilling rate at ER-PM contact sites formed by the CD4-Kv2.1FFAT motif chimera was only half as efficient as at sites formed by the full-length Kv2.1 channel (*SI Appendix*, Fig. S3*B*). This intermediate value suggests that simply forming ER-PM junctions does not confer efficient ER-Ca^{2+} uptake, and full-length Kv2.1 functionalizes the ER-PM junction with regard to Ca^{2+} handling. Taken together, our results confirm the canonical ionotropic role of Kv2.1 channels at the soma for regulating membrane voltage, while also revealing a nonconducting role for Kv2.1 in regulating ER Ca^{2+} filling during electrical activity or following ER store depletion.

Endogenous and Transfected Kv2.1 Localizes beyond the Somatodendritic Compartment into Axons and Presynaptic Compartments. Somatic Kv2.1 clearly regulates ER Ca^{2+} stores as illustrated in Fig. 1 and *SI Appendix*, Figs. S2 and S3. Since ER Ca^{2+} regulates axonal glutamate release (21), we wondered whether Kv2 channels could influence Ca^{2+} homeostasis, and thus glutamate release, in this neuronal compartment. To date, large Kv2 clusters have only been identified in the neuronal soma, proximal dendrites, and axon initial segment (31, 32, 40). However, given the smaller-size diameter (~1/10) of ER-PM junctions identified in distal axons (41), we sought to determine whether smaller clusters of Kv2.1 channels could be found localized in presynaptic sites.

We transfected neurons with green fluorescent protein (GFP)-Kv2.1 and Discosoma red fluorescent protein (dsRed)ER, followed by fixing and immunolabeling for synapsin. This reliably demonstrated forward trafficking of the GFP-Kv2.1 into punctate structures along the axon. As shown in Fig. 2*A*, the transfected Kv2.1 localized to presynaptic compartments identified by synapsin that were enriched in the ER luminal marker dsRedER. Moreover, we confirmed membrane insertion of exogenous Kv2.1 by coexpressing mRuby-Kv2.1 carrying an extracellular biotin-acceptor domain (BAD) with a biotin ligase, BirA. Successful labeling of the extracellular BAD with Alexa Fluor 488–conjugated streptavidin confirms that mRuby-Kv2.1loopBAD exits the axonal ER and is inserted into the PM (Fig. 2*B*).

Next, we immunostained for endogenous Kv2.1 within axons of our neuronal cultures and again detected Kv2.1 puncta in synapsin-positive presynaptic compartments of DIV 16 hippocampal cultures (see white arrows in Fig. 2*C*, *Inset*). The level of expression is much lower than that observed on the soma, and, if detected by investigators previously, was probably viewed as nonspecific antibody staining. To confirm the specificity of this staining, we used a two-strategy approach. First, we compared the intensity of the endogenous presynaptic Kv2.1 in neurons expressing Kv2.1 shRNA and found this signal reduced by similar amounts as in somas from the same cultures (*SI Appendix*, Fig. S4). In the second approach, we overexpressed a dominant-negative Kv2.1 (Kv2.1DN) subunit that solely consists of the Kv2.1 truncation including the first transmembrane domain. Kv2.1DN assembles with the endogenous Kv2.1 subunits and prevents forward trafficking out of the ER to the cell surface (*SI Appendix*, Fig. S5*A*). Kv2.1DN expression also blocked trafficking of Kv2.1 into detectable clusters within axonal compartments (see the outlined axon in *SI Appendix*, Fig. S5*B*). *SI Appendix*, Fig. S5*C* illustrates colocalization of the Kv2.1DN with synapsin, confirming expression throughout the cellular ER including in the axon, despite a lack of endogenous Kv2.1 detected in the axon. This dichotomy could be for a variety of reasons, including tetrameric assembly between endogenous and Kv2.1DN which may not leave the somatic ER. Alternatively, levels of endogenous Kv2.1 may now be at a low and homogenous distribution pushing them below the detection threshold by immunostaining. Note that the anti-Kv2.1 epitope resides in the channel C terminus which is lacking from the DN construct, so this antibody is only detecting endogenous levels.

To further confirm Kv2.1 expression in the axon, we examined AMIGO protein expression. AMIGO proteins are both adhesion molecules and Kv2 auxiliary β subunits (42, 43). To date, the only known mechanism for the localization of AMIGOs is their assembly with Kv2 channels. We identified small presynaptic clusters of endogenous AMIGO in hippocampal axons enriched with the presynaptic protein synapsin (*SI Appendix*, Fig. S5*D*). Additionally, we found that exogenous GFP-AMIGO localized to presynaptic terminals in control cells and that this presynaptic localization of the endogenous AMIGO was completely blocked when the Kv2.1DN was expressed (*SI Appendix*, Fig. S5*E* and *F*). Together, these three approaches validated the axonal immunolabeling. While exogenous expression sometimes causes proteins to mislocalize to intracellular compartments, this appears to not be the case, as both endogenous and transfected Kv2.1 and AMIGO were detected in presynaptic compartments.

Kv2.2 immunostaining was also detected weakly in both somatic and axonal compartments (*SI Appendix*, Fig. S6*A* and

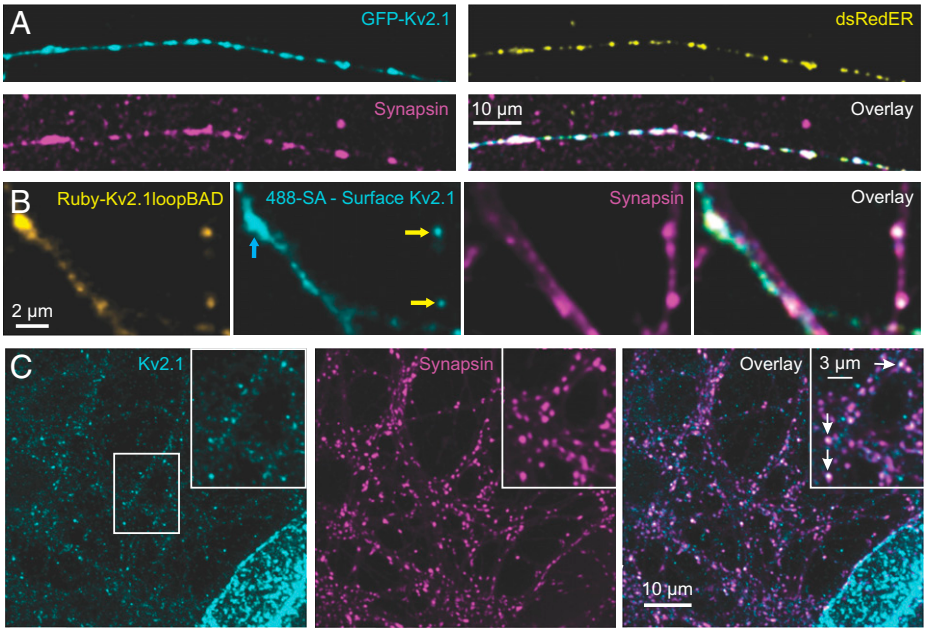

Fig. 2. Endogenous Kv2.1 localizes beyond the somatodendritic compartment into axons and terminals. (*A*) Images of transfected then fixed DIV 16 neurons expressing GFP-Kv2.1 (cyan) and dsRedER (yellow), with immunolabeled endogenous synapsin (magenta). (*B*) Images of a transfected neuron expressing Ruby-Kv2.1loopBAD (yellow), 488-streptavidin (SA) (cyan), and counterstained for synapsin (magenta). The streptavidin labeling was performed on live cells before fixation and synapsin immune-detection. Yellow arrows point to colocalization of synapsin with Ruby-Kv2.1loopBAD, indicating that Kv2.1 is surface localized at presynaptic compartments. Ruby-Kv2.1loopBAD is also readily found in dendrites (blue arrow) where synapsin colocalization is absent and streptavidin labeling confirms PM insertion. A single optical section is shown. (*C*) Immunolabeled images of endogenous Kv2.1 (cyan) and synapsin (magenta), with merged channels (*Right*), in DIV 14 neurons. The center white box indicates the region enlarged as shown in the *Inset*. Arrows indicate Kv2.1 colocalized with synapsin-positive presynaptic terminals.

B) and was also blocked by expressing Kv2.1DN (*SI Appendix*, Fig. S6*C* and *D*). Note that while some Kv2.2 immunostaining was present in presynaptic compartments (see white arrow in *SI Appendix*, Fig. S6*A*, *Inset*), it often appeared at a much lower level compared to Kv2.1, and Kv2.2 was at times not detected. In addition, Kv2.2 immunolabeling was often found adjacent to the synapsin puncta as opposed to fully colocalizing (see yellow arrowheads in *SI Appendix*, Fig. S6*A*, *Right*, *Inset*). Perhaps Kv2.2 predominates in postsynaptic (dendritic) compartments while present at a much lower level relative to Kv2.1 on the presynaptic side. However, given that the anti-Kv2.2 antibody is likely less efficient than its Kv2.1 counterpart, this issue remains an open question at this time. In summary, we were surprised to discover a population of smaller clusters of Kv2 channels that enrich in the distal axon at a majority of presynaptic terminals. This localization is not fully unexpected, however, given that ER-PM junctions have been reported in axon terminals (41) and the only known localization mechanism for Kv2 channels involves tethering to ER VAPs, which are prominent throughout the axonal ER.

Loss of Kv2.1 Impairs Axonal ER Ca^{2+} Influx during Stimulation Independent of Ion Conduction. We next investigated the functional role of axonal Kv2.1 channels. During our previous efforts to understand modulation of the AP waveform in cultured hippocampal neurons, we found that presynaptic terminals primarily rely on Kv1 and Kv3 channels to repolarize the AP (44). Consistent with this finding, optical recordings of axonal AP waveforms uncovered no difference in the amplitude or FWHM between control and Kv2.1 KD axons stimulated at 25 Hz (Fig. 3*A*–*C*). To further examine the role of Kv2.1 in the AP waveform over a range of physiological firing frequencies, we also made measurements of membrane voltage at both the axon and soma during AP trains delivered at 4 Hz. Once again, we saw no significant difference in either the amplitude or FWHM of APs in control or Kv2.1 KD neurons (*SI Appendix*, Fig. S7). Collectively, these results indicate that while Kv2.1 plays a prominent canonical role in the soma, it does not have a conducting role in the axon.

Next, we confirmed previous findings that the axonal ER robustly fills with Ca^{2+} during trains of stimulation (Fig. 3*D* and *E*). We found that the process of axonal ER Ca^{2+} filling during neuronal activity also appeared to rely on Kv2.1 channels, as neurons transfected with Kv2.1 shRNA had severely impaired in ER Ca^{2+} uptake during trains of stimulation (Fig. 3*F* and *G*). Further, ER filling from Kv2.1 KD was rescued by expressing an shRNA-resistant exogenous Kv2.1 with wobbled bases (wKv2.1; control neurons, 15.99 ± 2.22% ΔF/F; Kv2.1 KD neurons, 5.29 ± 0.71% ΔF/F; wKv2.1 neurons, 11.12 ± 1.92% ΔF/F) (Fig. 3*F* and *G*).

Since both Kv2.1 and Kv2.2 localized to presynaptic compartments where they form ER-PM junctions, we wanted to determine the level of contribution from total Kv2 channels to regulate axonal ER Ca^{2+}. We expressed Kv2.1DN to block insertion of both Kv2.1 and Kv2.2 in the PM (45). We found that impairing insertion of Kv2.1 and Kv2.2 channels also decreased axonal AP-evoked ER Ca^{2+} influx (control neurons, 18.17 ± 4.99% ΔF/F; Kv2.1 DN neurons, 3.18 ± 2.17% ΔF/F; $P < 0.05$) (Fig. 3*H* and *I*). These results suggest that Kv2.1 plays a critical role axonal ER Ca^{2+} influx without contributing a conducting role to repolarize the presynaptic AP.

Presynaptic Kv2.1 Modulates Neurotransmission Independently of Conduction. This striking nonionotropic role for axonal Kv2.1 channels in regulating ER Ca^{2+} filling during electrical activity was especially intriguing in light of recent work demonstrating that blocking SERCA pumps impairs neurotransmission (21). To explore a nonconducting role for Kv2.1 in modulating vesicle

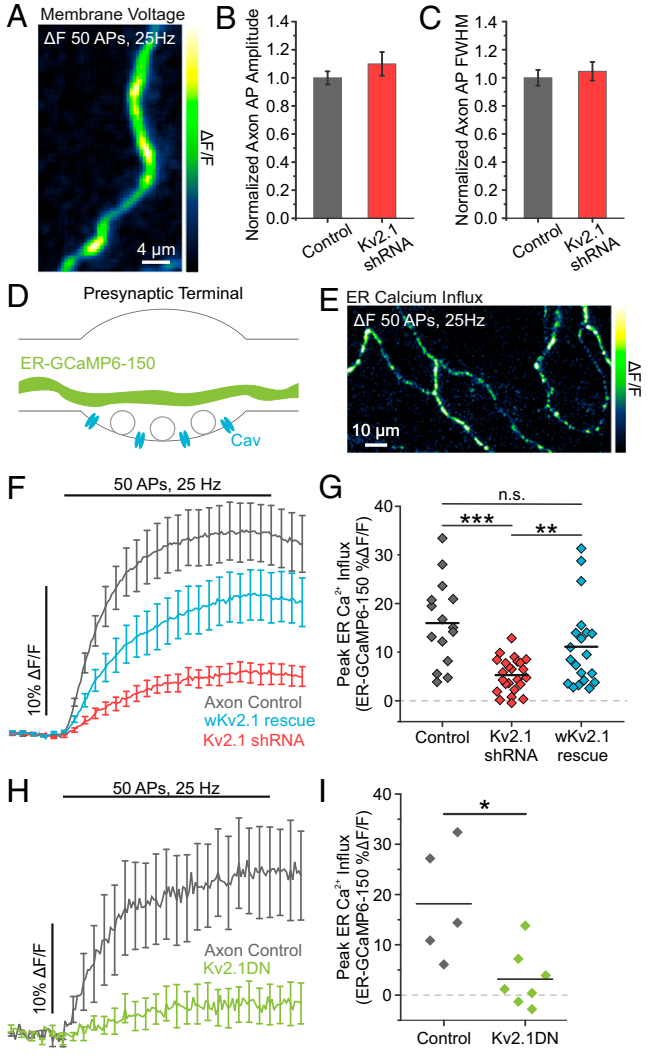

Fig. 3. Loss of Kv2.1 impairs axonal ER Ca^{2+} influx during stimulation. (*A*) Image of the change in fluorescence of axonal QuasAr in response to a train of 50 stimulations delivered at 25 Hz. (*B* and *C*) Quantification of AP amplitude (*B*) and FWHM (*C*) (control neurons, $n = 23$ cells; Kv2.1 KD neurons $n = 15$ cells). (*D*) Cartoon of a presynaptic terminal expressing the fluorescent Ca^{2+} indicator ER-GCaMP6-150 in the ER lumen. (*E*) Image of the change in fluorescence of axonal ER-GCaMP6-150 in response to a train of stimulation. (*F* and *G*) Average fluorescence traces of axonal ER-GCaMP6-150 (*F*) and quantification of peak fluorescence (*G*) for control, Kv2.1 KD, and wKv2.1 rescue neurons (control neurons, $n = 15$ cells; Kv2.1 KD neurons, $n = 24$ cells; wKv2.1 rescue neurons, $n = 20$ cells; $^{**}P < 0.01$, $^{***}P < 0.001$, Student's t test). n.s., not significant. (*H* and *I*) Average fluorescence traces of axonal ER-GCaMP6-150 (*H*) and quantification of peak fluorescence (*I*) for both control and Kv2.1 DN neurons (control neurons, $n = 5$ cells; Kv2.1 DN neurons, $n = 7$ cells; $^{*}P < 0.05$, Student's t test).

fusion, we used the pH-sensitive reporter of synaptic vesicle exocytosis (pHluorin) fused to the vesicular glutamate transporter (vGlut-pHluorin). vGlut-pHluorin signals are reported as a percentage of the total vesicle pool (% exocytosis), whose fluorescence is obtained by perfusion of a Tyrode's solution containing 50 mM NH_4Cl buffered at pH 7.4 (Fig. 4*A* and *B*) (46–49). Neurons transfected with Kv2.1 shRNA had a large (43.6%, $P < 0.0001$) reduction in exocytosis (Fig. 4*C* and *D*), similar to when Ca^{2+} uptake into the ER was blocked. These results suggest that Kv2.1 plays a significant nonconducting role in neurotransmission.

To confirm that this result was due to the loss of Kv2.1 protein rather than loss of a conducting, ionotropic, or voltage-sensing role, we turned to pharmacology. Kv2 channels detect membrane potential changes through a group of positive charges located in the S4 domain of the channel α subunit. We used the gating modifier Guangxitoxin-1E (GxTx) to block Kv2.1 voltage sensing and conduction. GxTx induces a depolarizing shift in the voltage-dependent activation of Kv2.1 with high potency and selectivity [IC_{50} (half maximal inhibitory concentration): 0.71 nM (50)]. Perfusion of 100 nM GxTx to prevent potassium conduction through Kv2.1 did not affect vGlut-pHluorin responses (Fig. 4*E* and *F*). Together with the finding that loss of Kv2.1 had no effect on axonal membrane voltage during an AP, these results further demonstrate that axonal Kv2.1 modulates neurotransmission independently of potassium conduction.

Reducing Kv2.1 expression impairs presynaptic Ca^{2+} influx. It was previously shown that chronically blocking SERCA pumps and ER Ca^{2+} uptake impairs Ca^{2+} influx from voltage-gated Ca^{2+} channels and vesicle fusion (21). We sought to determine if the loss of Kv2.1-based ER Ca^{2+} refilling during electrical activity also impairs AP-evoked increases in cytosolic Ca^{2+}. We found that depletion of Kv2.1 altered presynaptic Ca^{2+} influx during trains of stimulation using the fluorescent Ca^{2+} indicator GCaMP6f fused to synaptophysin (51, 52) (SypGCaMP6f) (Fig. 5*A* and *B*). Not surprisingly, compared to controls, neurons cotransfected with SypGCaMP6f and Kv2.1 shRNA had reduced presynaptic Ca^{2+} influx when stimulated with 50 APs

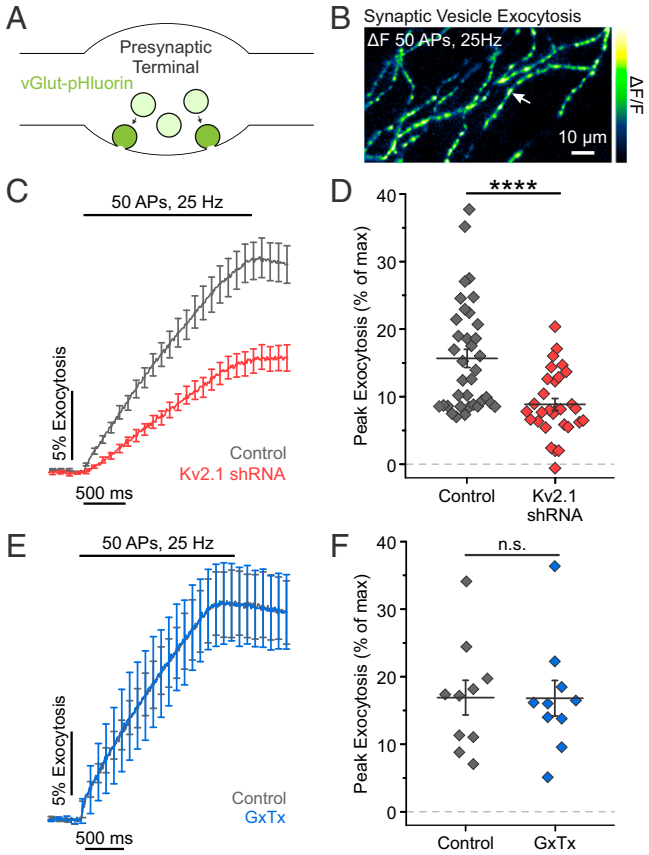

Fig. 4. Presynaptic Kv2.1 modulates neurotransmission independently of conduction. (*A*) Cartoon of a presynaptic terminal containing synaptic vesicles expressing vGlut-pHluorin, a pH-sensitive indicator of exocytosis. (*B*) Image of the change in fluorescence of vGlut-pHluorin in response to a train of stimulation. The arrow marks the example location of presumptive presynaptic terminals. (*C* and *D*) Average fluorescence traces of vGlut-pHluorin (*C*) and quantification of peak fluorescence (*D*) for both control and Kv2.1 KD neurons (control neurons, $n = 36$ cells; Kv2.1 KD neurons, $n = 30$ cells; $^{****}P < 0.0001$, Student's t test). (*E* and *F*) Average fluorescence traces of vGlut-pHluorin (*E*) and quantification of peak fluorescence (*F*) for neurons ± GxTx ($n = 10$ cells, paired t test). n.s., not significant.

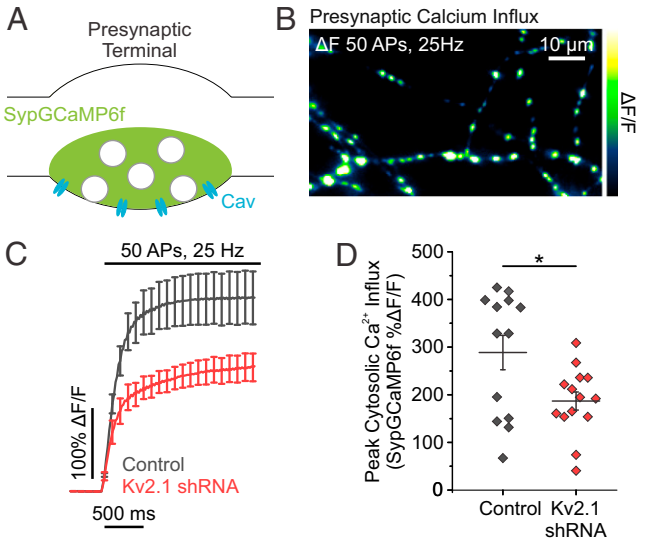

Fig. 5. Reducing Kv2.1 expression impairs evoked presynaptic Ca^{2+} influx. (*A*) Cartoon of a presynaptic terminal expressing the fluorescent Ca^{2+} indicator Synaptophysin-GCaMP6f (SypGCaMP6f). (*B*) Image of the change in fluorescence of SypGCaMP6f in response to a train of stimulation. (*C* and *D*) Average fluorescence traces of SypGCaMP6f (*C*) and quantification of peak fluorescence (*D*) in both control and Kv2.1 KD neurons (control neurons, $n = 13$ cells; Kv2.1 KD neurons, $n = 14$ cells; $^*P < 0.05$, Student's t test).

delivered at 25 Hz (control neurons, 288.60 ± 36.06% ΔF/F; Kv2.1 KD neurons 186.84 ± 18.99% ΔF/F; $P < 0.05$) (Fig. 5*C* and *D*). Thus, the loss of Kv2.1 phenocopies the effects of blocking SERCA pumps with CPA. CPA not only blocks Ca^{2+} influx but also impairs resting levels of ER luminal Ca^{2+}, which triggers STIM1 oligomerization that could impair synaptic transmission (21). STIM1 oligomerization has two effects with regard to Ca^{2+} entry: 1) it activates Orai to form a CRAC (53), and 2) it can impair voltage-gated Ca^{2+} channels (54). The latter is suspected to impair exocytosis when ER stores are depleted (21). To determine if the loss of Kv2.1 impairs exocytosis through activation of STIM1, we utilized shRNA to KD expression levels of both Kv2.1 and STIM1. Compared to Kv2.1 KD neurons, neurons cotransfected with Kv2.1 shRNA and STIM1 shRNA had no difference in the magnitude of vesicle fusion (Kv2.1 KD neurons, 6.39 ± 2.17% exocytosis; Kv2.1 KD + STIM1 KD neurons, 7.83 ± 2.01% exocytosis) (*SI Appendix*, Fig. S8), indicating that ER Ca^{2+} sensing is not limiting vesicle fusion with Kv2.1 knockdown. These results suggest that disabling ER Ca^{2+} uptake through Kv2.1 KD impairs exocytosis through a pathway independent of STIM1 activation, despite strongly matching the phenotype blocking SERCA pumps using CPA.

The Kv2.1 Channel C Terminus Is Necessary for Maintaining Synaptic Transmission. We next addressed the mechanism underlying Kv2.1's role in ER Ca^{2+} handling and neurotransmission by conducting rescue experiments. We found that expression of the shRNA-resistant wKv2.1 was able to restore exocytosis in the Kv2.1 KD background to values similar to control neurons (Kv2.1 KD neurons, 6.29 ± 0.89%; wKv2.1 rescue neurons, 12.22 ± 2.40% exocytosis; $P < 0.05$) (Fig. 6*A*–*C*). The formation of ER-PM junctions by Kv2.1 channels in the PM occurs via a noncanonical VAP-binding motif within the C-terminal tail of Kv2.1 (11, 37); deletion or mutation of this motif abolishes Kv2.1 clusters and ER-PM junctions (35, 40). However, despite a lack of clustering, the loss of the C-terminal tail does not alter Kv2.1's electrical function (6, 55). Not surprisingly, without the C-terminal tail that enables VAP binding and clustering of the Kv2.1 channel, we could no longer visualize Kv2.1 punctate structures in the soma or axon. Moreover, expressing Kv2.1 with a truncated C terminus (Kv2ΔC318) in the Kv2.1 KD background was also unable to restore synaptic transmission (Kv2.1 KD neurons, 7.49 ± 0.72%; Kv2ΔC318 neurons, 9.28 ± 1.21% exocytosis) (Fig. 6*D*–*F*). Next, we were curious if the C terminus alone is sufficient to restore synaptic function. To distinguish between the specialized Kv2.1 ER-PM junctions and simply bringing ER and PM membranes together through the VAP-binding domain, we returned to the CD4-Kv2.1FFAT chimera used in *SI Appendix*, Fig. S3. Expression of the CD4-Kv2.1FFAT was localized to the presynaptic terminals (*SI Appendix*, Fig. S9); however, it was not sufficient to restore exocytosis to control levels in Kv2.1 KD neurons (Kv2.1 KD neurons, 6.41 ± 1.35%; CD4-Kv2.1FFAT neurons, 7.45 ± 1.98% exocytosis) (Fig. 6*G*–*I*). This result indicates that other sequences within Kv2.1 are required to enable efficient ER Ca^{2+} uptake that can support synaptic transmission, rather than acting simply to recruit VAP. Further, this observation is in agreement with our finding of much less efficient ER-Ca^{2+} uptake after store depletion when expressing CD4-Kv2.1FFAT instead of full-length Kv2.1 (*SI Appendix*, Fig. S3). At the same time, Kv2.1 clustering and inclusion of the VAP-binding motif is essential, as expressing Kv2.1 with a truncated C terminus (Kv2ΔC318) was also unable to restore synaptic transmission. Taken together, these results support the role of Kv2.1 as an essential hub protein that acts through a novel mechanism to enable the efficient ER Ca^{2+} uptake during electrical stimulation that is required to maintain neurotransmitter release.

Discussion

In most cells, the ER acts mainly as a Ca^{2+} source in the cytosol commonly exploited by different pathways that activate ryanodine receptors or inositol 1,4,5-trisphosphate receptors. Intriguingly, the neuronal ER acts as a net Ca^{2+} sink in both the soma and axon of neurons, using SERCA pumps to extract Ca^{2+} from small microdomains in the cytosol formed by the opening of voltage-gated Ca^{2+} channels. Inhibiting the activity of SERCA during electrical activity has previously been demonstrated to dramatically impair synaptic function (56, 57). To date, a mechanism that enables efficient access of SERCA to transient sources Ca^{2+} from PM voltage-gated Ca^{2+} influx has not been identified. Here, we provide evidence that the nonconducting signaling hubs of Kv2.1 channels enable an elegant coupling of Ca^{2+} uptake into the ER during electrical activity in both the soma and synaptic terminals (Figs. 1 and 3). Loss of Kv2.1 renders the ER unable to extract Ca^{2+} from the cytosol during electrical activity and makes the neuron behave as if the SERCA pumps are not functional during stimulation. Interestingly, the loss of Kv2.1 channels matches the phenotypes of the SERCA block with respect to impaired cytosolic Ca^{2+} influx and vesicle fusion during electrical stimulation (Figs. 4 and 5).

This interesting phenotype of impaired AP-evoked Ca^{2+} influx was also reported by another group when they knocked down VAP protein using shRNA (58). Our results support the necessity of Kv2.1-VAP ER-PM junctions, as the loss of the C-terminal VAP-binding domain was unable to restore synaptic transmission (Fig. 6). Although a CD4 chimera containing the Kv2.1 C terminus was shown to recruit VAP and form ER-PM junctions in neurons and heterologous cells (11), it was not

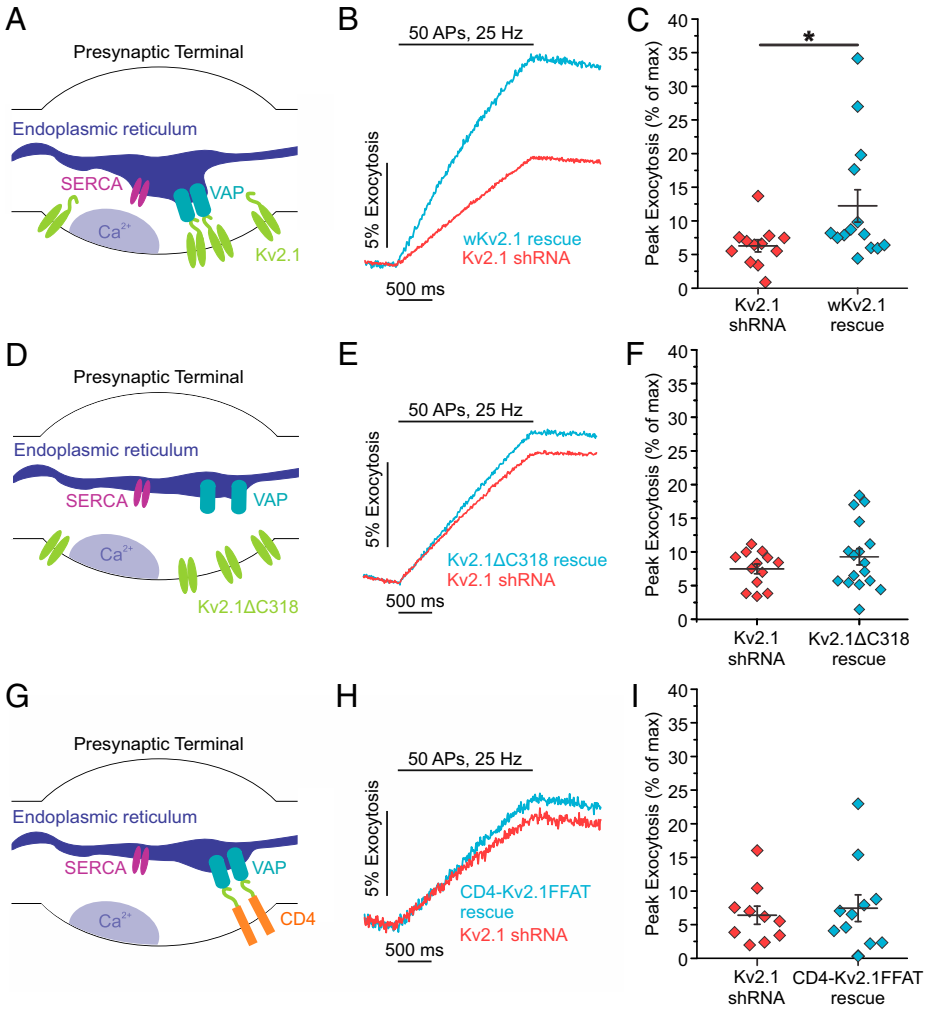

Fig. 6. The VAP-binding domain on Kv2.1 is necessary but not sufficient to rescue synaptic vesicle exocytosis. (*A*) Cartoon of a presynaptic terminal with endogenous Kv2.1 channels tethering the ER to the PM, positioning SERCA pumps nearby to a source of presynaptic Ca^{2+} influx. (*B* and *C*) Average fluorescence traces of vGlut-pHluorin (*B*) and quantification of peak fluorescence (*C*) in both Kv2.1 and shRNA-resistant (wobbled) Kv2.1 rescue neurons (Kv2.1 KD neurons, $n = 12$ cells; wKv2.1 rescue neurons, $n = 14$ cells; $^*P < 0.05$, Student's t test). (*D*) Cartoon of a presynaptic terminal expressing mCherry-Kv2ΔC318, which is missing the Kv2.1 VAP-binding domain and does not localize SERCA near sites of presynaptic Ca^{2+} influx. (*E* and *F*) Average fluorescence traces of vGlut-pHluorin (*E*) and quantification of peak fluorescence (*F*) in both Kv2.1 shRNA and Kv2ΔC318 rescue neurons (Kv2.1 KD neurons, $n = 13$ cells; Kv2ΔC318 neurons, $n = 17$ cells). (*G*) Cartoon of a presynaptic terminal expressing the CD4-Kv2.1FFAT chimera, which creates ER-PM junctions perhaps in alternate locations away from sites of presynaptic Ca^{2+} influx. (*H* and *I*) Average fluorescence traces of vGlut-pHluorin (*H*) and quantification of peak fluorescence (*I*) in both Kv2.1 shRNA and CD4-Kv2.1FFAT rescue neurons (Kv2.1 KD neurons, $n = 10$ cells; CD4-Kv2.1FFAT neurons, $n = 11$ cells).

able to restore synaptic transmission and poorly supported somatic ER Ca^{2+} refilling (Fig. 6 and *SI Appendix*, Fig. S3). While resolution limitation in fluorescence microscopy precludes us from making precise measurements of subsynaptic localization differences between Kv2.1 and CD4-Kv2.1FFAT, our results suggest that Kv2.1 truly acts a hub either by localizing sites of Ca^{2+} entry or through other interactions to position ER-PM junctions specifically proximal to Ca^{2+} entry to promote synaptic transmission (Fig. 6). Taken together, these results support a nonconducting role for the Kv2.1 channel as a hub protein to couple ER Ca^{2+} handling with electrical activity essential for neuronal function. Kv2.1 has also been identified to play a nonconducting role in exocytosis/secretion in other cells, especially those that are electrically active, e.g., insulin release in pancreatic beta cells (6), although a role for modulating the ER's Ca^{2+} handing was not explored in those studies.

It is surprising that blocking a mechanism of Ca^{2+} extrusion from the cytosol could negatively regulate the Ca^{2+}-dependent process of vesicle fusion. This same dichotomy was reported when SERCA pump function was blocked using the drug CPA, which also depletes resting levels of ER Ca^{2+}. In the case of CPA exposure, STIM1 was the reported mechanism for blocking exocytosis and voltage-gated Ca^{2+} channels (21). However, here we do not find that STIM1 appears to be triggered to block exocytosis (*SI Appendix*, Fig. S8) with decreased expression of Kv2.1. This could be that the loss of Kv2.1 selectively impairs ER filling during activity but ultimately does not regulate resting levels of ER Ca^{2+}. Alternatively, the other STIM isoform (STIM2) may act as a more dominant sensor. We would also not rule out the possibility that Kv2 ER-PM junctions recruit other critical proteins which may or may not rely on unique Ca^{2+} handling between the ER and PM.

To date, the most well-known ER-PM junction with respect to Ca^{2+} handling is formed between isoforms of the ER lumen Ca^{2+}-sensor STIM and the Ca^{2+} channel Orai, which are the fundamental working machinery of the CRAC channel. In the classical pathway for SOCE, the CRAC channel is formed only when the ER lumen Ca^{2+} concentration is dramatically depleted and transiently exists until the ER lumen is filled. Kv2.1 could also enhance this process, as suggested by the somatic ER refilling

data in *SI Appendix*, Fig. S3. However, in the context of neuronal signaling, the process of activating a CRAC channel is rather slow and can cause Ca^{2+} spillover into the cytosol when activated; it is difficult to imagine neurons relying on this mechanism alone to maintain ER Ca^{2+}. Indeed, chronic activation of CRAC channels was found to up-regulate spontaneous vesicle fusion (59). Additionally, activation of STIM appears to inhibit or activate a number of PM proteins (60), although interestingly, even with KD of STIM1 by shRNA, the ER is still able to influx Ca^{2+} during stimulation (21). Thus, although STIM and Orai can replenish ER stores when the ER lumen is severely depleted of Ca^{2+}, an "on-demand" mechanism to efficiently keep the ER filled and coupled to electrical activity solves several problems without perturbing additional novel sources of Ca^{2+} entry and spillover. In this way, the Kv2.1-VAP ER-PM junctions are different from those formed by STIM/CRAC channels because they are engaged independent of ER lumen Ca^{2+} levels. Interestingly, Kv2.1 clusters are dynamic in some situations and can be dispersed in hypoxic or ischemic conditions such as a stroke (61, 62) or when exposed to high levels of extracellular glutamate (12, 61, 63). This insult-induced unbinding of Kv2.1 from the ER membrane may be quite useful for limiting neurotransmitter release under certain pathological conditions and clearly merits additional experiments.

Why form ER-PM junctions with a voltage-sensitive protein? The movement of the positive charges within the voltage sensor during membrane depolarization produces a gating current that precedes and is independent of ion conduction during channel opening. It is possible that electrically excitable cells could be using Kv2.1 as a voltage sensor to communicate changes in membrane potential across the ER-PM junction. Indeed, the charge movement of the voltage sensor in L-type Ca^{2+} channels communicates to ryanodine receptors in mammalian skeletal muscle during excitation-contraction coupling (64, 65). Although we cannot fully rule out communication of charge movement from Kv2.1 to the ER initiating Ca^{2+} uptake, it seems unlikely as our use of the gating modifier GxTx, which should block both voltage-sensing and conduction, did not impair neurotransmission. It has also been shown that ion channels have preferred lipid environments, and Kv2.1 clusters could define the local lipid environment to recruit additional channels and proteins for crucial interactions at the site of ER-PM junctions.

As the Kv2.1-VAP–mediated ER-PM junction allows the ER to quickly access Ca^{2+} during electrical activity, a key question remains as to what the ER is doing with the additional Ca^{2+}. Here, we would argue that it is likely not just to prevent severe depletion, duplicating the role of SOCE. It has been proposed that an essential role of the ER is to shuttle Ca^{2+} to other organelles, including into mitochondria via the Ca^{2+} uniporter (MCU), which has different affinities for Ca^{2+} depending on subunit expression. A recently identified MICU3 subunit is required for neuronal mitochondria to receive Ca^{2+} from the cytosol (66), but it remains unclear if they also receive Ca^{2+} from the ER to couple electrical activity to ATP production. A second possibility is that the ER may be shuttling Ca^{2+} to other organelles or Ca^{2+}-sensitive proteins. Indeed, the cytosol of the neuron is a highly buffered Ca^{2+} environments identified; thus, a mechanism to coordinate Ca^{2+} delivery to microdomains within the cytoplasm may be very useful for coupling Ca^{2+}-signaling to protein activation in distal processes of neurons like the axon. One example is seen in *Drosophila*, where ER Ca^{2+} is used to activate calcineurin, a Ca^{2+}-dependent phosphatase, in an essential role for synapse development (67). Interestingly, calcineurin has been shown to impact channel clustering by dephosphorylating several sites on Kv2.1, including the FFAT VAP-binding motif (61). Future studies looking at this influence on neurotransmission could further elucidate a dynamic role for ER-PM junctions in synaptic function. Alternatively, rather than acting to move Ca^{2+} between organelles, the ER may be polarized within the neuron and take in Ca^{2+} during electrical stimulation, which may then be released at other subcellular locations within the soma or axon. As the dynamics of ER Ca^{2+} are not static, our identification of an on-demand mechanism for ER Ca^{2+} filling during electrical stimulation opens avenues of research to understand ER signaling in neurons.

Materials and Methods

Cell Culture and Transfection. Primary neurons from Sprague-Dawley rats of either sex on postnatal day 0 to 1 were cultured for all experiments. Briefly, hippocampal CA1 to CA3 regions with the dentate gyri removed were harvested, tissue was dissociated into single cells with bovine pancreas trypsin, and cells were plated onto poly-L-ornithine–coated glass coverslips inside a 6-mm cloning cylinder. Ca^{2+} phosphate–mediated DNA transfection was performed on cultures at 5 to 6 DIV. In some cases, GFP-Kv2.1 and dsRedER were transfected using Lipofectamine 2000 (Life Technologies) as previously described (12). Methods regarding biotinylation of surface Kv2.1 and use of the GFP-AMIGO have been previously described (9, 68). All experiments were performed on mature neurons between 14 and 24 DIV. To ensure reproducibility, experiments were performed on neurons from a minimum of three separate cultures. All protocols used were approved by the Institutional Animal Care and Use Committee at Dartmouth College and conform to the NIH Guidelines for the Care and Use of Animals.

Genetic Tools. The following constructs were used: QuasAr2 (variant DRH334, hSyn promoter) (29), vGlut-pHluorin (46), SypGCaMP6f (51, 52), ER-GCaMP6-150 (Addgene #86918) (21), CD4-Kv2.1FFAT (11), and mGreenLantern (Addgene #161912) (34). To reduce endogenous Kv2.1 expression for live cell imaging, an shRNA plasmid was obtained from OriGene against the following mRNA target sequence: CAGAGTCCTCCATCTACACCACAGCAAGT. STIM1 shRNA was also purchased from OriGene (TR707032, variant C). For rescue experiments in Kv2.1 KD neurons, three silent mutations were introduced into the rat Kv2.1 sequence to generate the "wobbled" Kv2.1 (wKv2.1) construct: C2154T, C2157A, and C2160T.

Live Cell Imaging. All experiments were performed at 34 °C using a custom-built objective heater. Cultured cells were mounted in a rapid-switching laminar flow perfusion and stimulation chamber on the stage of a custom-built epifluorescence microscope. Neurons were perfused at a rate of 400 μL/min in a modified Tyrode's solution containing the following: 119 mM NaCl, 2.5 mM KCl, 2 mM $CaCl_2$, 2 mM $MgCl_2$, 25 mM Hepes, and 30 mM glucose with 10 μM cyanquixaline (Sigma-Aldrich) and 50 μM AP5 (Sigma-Aldrich). Images were obtained using either a Zeiss Observer Z1 equipped with an EC Plan-Neofluar 40× 1.3 numerical aperture (NA) oil immersion objective or an Olympus IX-83 microscope equipped with a 40× 1.35 NA oil immersion objective (UApoN40XO340-2). All images were captured with an IXON Ultra 897 Electron Multiplying Charge Coupled Device (EMCCD) (Andor) that was cooled to −80 °C by an external liquid cooling system (EXOS). All excitation light occurred via OBIS lasers (Coherent). APs were evoked by passing 1-ms current pulses yielding fields of ∼12 V/cm^2 via platinum/iridium electrodes. Timing of stimulation was delivered by counting frame numbers from a direct readout of the EMCCD rather than time itself for more exact synchronization using a custom-built board powered by an Arduino Duo chip manufactured by an engineering firm (Sensorstar).

Voltage measurements. QuasAr fluorescence was recorded with a 980-μs exposure time; images were acquired at 1 kHz using an OptoMask (Cairn Research) to prevent light exposure of nonrelevant pixels. Cells were illuminated with 70 to 120 mW by an OBIS 637-nm laser (Coherent) with ZET635/20x, ET655lpm, and ZT640rdc filters (Chroma).

Cytosolic Ca^{2+} measurements. GCaMP6f fluorescence was recorded with a 29.5-ms exposure time and images were acquired at 30 Hz. Cells were illuminated by an OBIS 488-nm laser at 7 to 9 mW (Coherent) with ET470/40x, ET525/50 m, and T495lpxr filters (Chroma). We repeated and averaged three to four trials to measure AP train stimulation-induced responses.

ER Ca^{2+} measurements. ER-GCaMP6-150 fluorescence was recorded with a 19.8-ms exposure time and images were acquired at 50 Hz. Cells were illuminated by an OBIS 488-nm laser at 7 to 9 mW for axonal recordings and at 1 to 2 mW for somatic recordings (Coherent) with ET470/40x, ET525/50 m, and T495lpxr filters (Chroma). We repeated and averaged three to four trials measuring AP train stimulation-induced responses.

Vesicle fusion measurements. vGlut-pHluorin fluorescence was captured with an exposure time of 9.8 ms and images were acquired at 100 Hz. Cells were illuminated by an OBIS 488-nm laser at 7 to 9 mW (Coherent) with ET470/40x, ET525/50 m, and T495lpxr filters (Chroma). For Guangxitoxin experiments, GxTx was continuously perfused at 100 nm (Alomone Labs). Cells were bathed in 50 mM NH_4Cl to neutralize vesicle pH at the end of each experiment to quantify vesicle fusion.

Immunocytochemistry.

To validate the effectiveness of our KD strategy. Neurons were fixed with 4% paraformaldehyde and 4% sucrose in phosphate-buffered saline (PBS) for 10 min, permeabilized with 0.2% Triton X-100 for 10 min, and blocked with 5% goat serum in PBS for 30 min at room temperature. Neurons were then incubated with the Kv2.1 primary antibody K89/34 (NeuroMab) and a GFP primary antibody (A10262, Invitrogen) overnight at 4 °C. Cells were washed three times with PBS and incubated for 1 h with Alexa Fluor–conjugated secondary antibodies (Invitrogen).

To detect the localization of endogenous Kv2 channels and AMIGO. Hippocampal cultures of neurons were isolated from E18 Sprague-Dawley rat brains of both sexes. Pregnant rats were deeply anesthetized with isoflurane, as outlined in a protocol approved by the Institutional Animal Care and Use Committee of Colorado State University (protocol ID 15-6130A). Hippocampi were dissociated and cultured as previously described for neurons (69, 70). Cultures were seeded on glass-bottom 35-mm dishes [with No. 1.5 coverslips (MatTek)] coated with poly-L lysine (Sigma-Aldrich) in borate buffer and in a medium composed of Neurobasal (Gibco/Thermo Fisher Scientific), B27 Plus Supplement (Gibco/Thermo Fisher Scientific), penicillin/streptomycin (Cellgro/Mediatech), and GlutaMAX (Gibco/Thermo Fisher Scientific).

Cultures of the indicated DIV were fixed with 4% formaldehyde for 15 min at room temperature in neuronal imaging saline (NIS) composed of 126 mM NaCl, 4.7 mM KCl, 2.5 mM $CaCl_2$, 0.6 mM $MgSO_4$, 0.15 mM NaH_2PO_4, 0.1 mM ascorbic acid, 8 mM glucose, and 20 mM Hepes, pH 7.4, 300 mOsm. Following six washes with NIS, the fixed cells were blocked in NIS with 10% goat serum and 0.1% Triton X-100 for 4 to 10 h at room temperature. Purified Kv2 and AMIGO mouse monoclonal antibodies, knockout verified, were from NeuroMab (Kv2.1, K89/34; Kv2.2, N37B/1; and AMIGO, L86A/37) were used in respective individual trials at a 1/1,000 dilution in NIS with 10% goat serum and 0.1% Triton X-100 for 1 h at room temperature followed by three 5-min washes in NIS and then a 45-min secondary antibody (1/2,000 dilution) incubation at room temperature in NIS with 10% goat serum and 0.1% Triton X-100. The Alexa Fluor 488–conjugated goat anti-mouse IgG (A11001) secondary antibody was from Invitrogen. Cells were then rinsed three times for 5 min each, immediately mounted under glass coverslips with Aqua-Poly/Mount (Polysciences), and imaged as described below. Synapsin 1/2 rabbit polyclonal antibody (002 106) was obtained from Synaptic Systems and used at 1/2,000 as described earlier except that here the secondary antibody was Alexa Fluor 647–conjugated goat anti-rabbit IgG (A21244), also from Invitrogen. When quantitating shRNA knockdown of presynaptic Kv2.1, a chicken anti-GFP antibody (A10262, Invitrogen) was used to localize the vGlut-pHluorin, given that fixation does lower the pHluorin florescence. Here an AlexaFluor488–conjugated anti-chicken secondary antibody (Invitrogen) was also used. Other immunodetection details are presented in the figure legends.

Spinning disk confocal microscopy was performed on immunolabeled cultures using a Yokogawa-based CSUX1 system with an Olympus IX83 inverted stand and coupled to an Andor laser launch containing 405-, 488-, 568-, and 637-nm diode lasers, 100 to 150 mW each. Images were collected using an Andor iXon EMCCD camera (DU-897) and 100× Plan Apo, 1.4 NA objective. To prevent bleed over between fluorescent channels, all imaging was performed sequentially with paired excitation-emission filter settings. This confocal system uses MetaMorph software (version 7.8.13.0). Image analysis and presentation was performed using Volocity v6.1.1 software, and all presented images were filtered and adjusted for brightness and contrast.

Western Blotting. To verify the efficiency of Kv2.1 KD, hippocampal neurons were treated at DIV 3 with AAV1-mCherry-pU6-Kv2.1 shRNA designed by OriGene (target sequence: CAGAGTCCTCCATCTACACCACAGCAAGT) and produced by Vector Biolabs. Untreated neurons were used as a control. At DIV 19, control and Kv2.1 shRNA virus-treated neurons were extracted in radioimmunoprecipitation assay buffer (50 mM Tris, pH 8.0, 150 mM NaCl, 1% Nonidet P-40, 0.5% sodium deoxycholate, and 0.1% SDS supplemented with protease inhibitors) for 1 h at 4 °C. The lysates were centrifuged at 13,000 × *g* at 4 °C for 10 min, and the protein concentrations were measured with bicinchoninic acid assays. The proteins were loaded and run on sodium dodecyl sulfate–polyacrylamide gel electrophoresis (SDS-PAGE) gels, transferred to polyvinylidene difluoride (PVDF) membranes, and immunoblotted with anti-Kv2.1 antibody (K89/34, NeuroMab) and anti–α-tubulin antibody (Sigma). The blots were detected using chemiluminescence reagent on a Bio-Rad Chemidoc MP and ImageJ was used for quantification of detected bands.

Image and Data Analysis. Images were analyzed in ImageJ using a custom-written plugin (rsb.info.nih.gov/ij/plugins/time-series.html). To quantify fluorescence, we selected 1.4-μm-diameter circular regions of interest (ROIs) from ΔF images of each experiment, recentering on the brightest pixel within the ROI in the ΔF image. ROIs were selected based on localized responses of voltage, Ca^{2+}, or vesicle fusion, rather than morphology, to define a presynaptic terminal. All statistical data are presented as means ± SEM (n = number of neurons) and all experiments were performed on more than three independent cultures. To measure the FWHM of QuasAr fluorescence, we used Origin version 9.1 (Origin Lab). Quantification of vesicle fusion was obtained by normalizing the fluorescence change in response to stimulation to the total number of vesicles measured by application of ammonium chloride.

Quantification and Statistical Analysis. Statistical analyses were performed in Excel and Origin. We used the paired two-sample for means *t* test for paired results. Normally distributed data were processed with the Student's *t* test for two independent distributions.

Data Availability. All study data are included in the article and/or *SI Appendix*.

ACKNOWLEDGMENTS. This work was supported by the Esther A. and Joseph Klingenstein Fund (M.B.H.), NIH National Institute of Neurological Disorders and Stroke Grants F31NS110192 (L.C.P.) and 1R01NS112365 (M.M.T. and M.B.H.), the National Science Foundation Integrative Organismal Systems 1750199 (I.H.C.), and National Institute of General Medical Sciences Grant P20GM113132 (M.B.H.).

1. S. Pal, K. A. Hartnett, J. M. Nerbonne, E. S. Levitan, E. Aizenman, Mediation of neuronal apoptosis by Kv2.1-encoded potassium channels. *J. Neurosci.* **23**, 4798–4802 (2003).
2. S. A. Malin, J. M. Nerbonne, Delayed rectifier K+ currents, IK, are encoded by Kv2 alpha-subunits and regulate tonic firing in mammalian sympathetic neurons. *J. Neurosci.* **22**, 10094–10105 (2002).
3. H. Murakoshi, J. S. Trimmer, Identification of the Kv2.1 K+ channel as a major component of the delayed rectifier K+ current in rat hippocampal neurons. *J. Neurosci.* **19**, 1728–1735 (1999).
4. J. Du, L. L. Haak, E. Phillips-Tansey, J. T. Russell, C. J. McBain, Frequency-dependent regulation of rat hippocampal somato-dendritic excitability by the K+ channel subunit Kv2.1. *J. Physiol.* **522**, 19–31 (2000).
5. K. M. O'Connell, R. Loftus, M. M. Tamkun, Localization-dependent activity of the Kv2.1 delayed-rectifier K+ channel. *Proc. Natl. Acad. Sci. U.S.A.* **107**, 12351–12356 (2010).
6. J. Fu *et al.*, Kv2.1 clustering contributes to insulin exocytosis and rescues human β-cell dysfunction. *Diabetes* **66**, 1890–1900 (2017).
7. D. A. Jacobson *et al.*, Kv2.1 ablation alters glucose-induced islet electrical activity, enhancing insulin secretion. *Cell Metab.* **6**, 229–235 (2007).
8. D. Greitzer-Antes *et al.*, K_v2.1 clusters on β-cell plasma membrane act as reservoirs that replenish pools of newcomer insulin granule through their interaction with syntaxin-3. *J. Biol. Chem.* **293**, 6893–6904 (2018).
9. E. Deutsch *et al.*, Kv2.1 cell surface clusters are insertion platforms for ion channel delivery to the plasma membrane. *Mol. Biol. Cell* **23**, 2917–2929 (2012).
10. N. C. Vierra, M. Kirmiz, D. van der List, L. F. Santana, J. S. Trimmer, Kv2.1 mediates spatial and functional coupling of L-type calcium channels and ryanodine receptors in mammalian neurons. *eLife* **8**, e49953 (2019).
11. B. Johnson *et al.*, Kv2 potassium channels form endoplasmic reticulum/plasma membrane junctions via interaction with VAPA and VAPB. *Proc. Natl. Acad. Sci. U.S.A.* **115**, E7331–E7340 (2018).
12. P. D. Fox *et al.*, Induction of stable ER-plasma-membrane junctions by Kv2.1 potassium channels. *J. Cell Sci.* **128**, 2096–2105 (2015).

13. M. West, N. Zurek, A. Hoenger, G. K. Voeltz, A 3D analysis of yeast ER structure reveals how ER domains are organized by membrane curvature. *J. Cell Biol.* **193**, 333–346 (2011).
14. S. Carrasco, T. Meyer, STIM proteins and the endoplasmic reticulum-plasma membrane junctions. *Annu. Rev. Biochem.* **80**, 973–1000 (2011).
15. Y. J. Chen, C. G. Quintanilla, J. Liou, Recent insights into mammalian ER-PM junctions. *Curr. Opin. Cell Biol.* **57**, 99–105 (2019).
16. D. E. Clapham, Calcium signaling. *Cell* **131**, 1047–1058 (2007).
17. G. L. Koch, The endoplasmic reticulum and calcium storage. *BioEssays* **12**, 527–531 (1990).
18. G. Montenegro *et al.*, Mutations in the ER-shaping protein reticulon 2 cause the axon-degenerative disorder hereditary spastic paraplegia type 12. *J. Clin. Invest.* **122**, 538–544 (2012).
19. M. P. Mattson, K. J. Tomaselli, R. E. Rydel, Calcium-destabilizing and neurodegenerative effects of aggregated beta-amyloid peptide are attenuated by basic FGF. *Brain Res.* **621**, 35–49 (1993).
20. D. Chattopadhyay, S. Sengupta, First evidence of pathogenicity of V234I mutation of hVAPB found in amyotrophic lateral sclerosis. *Biochem. Biophys. Res. Commun.* **448**, 108–113 (2014).
21. J. de Juan-Sanz *et al.*, Axonal endoplasmic reticulum Ca^{2+} content controls release probability in CNS nerve terminals. *Neuron* **93**, 867–881.e6 (2017).
22. M. Maletic-Savatic, N. J. Lenn, J. S. Trimmer, Differential spatiotemporal expression of K+ channel polypeptides in rat hippocampal neurons developing in situ and in vitro. *J. Neurosci.* **15**, 3840–3851 (1995).
23. M. Martina, J. H. Schultz, H. Ehmke, H. Monyer, P. Jonas, Functional and molecular differences between voltage-gated K+ channels of fast-spiking interneurons and pyramidal neurons of rat hippocampus. *J. Neurosci.* **18**, 8111–8125 (1998).
24. K. J. Rhodes, S. A. Keilbaugh, N. X. Barrezueta, K. L. Lopez, J. S. Trimmer, Association and colocalization of K+ channel alpha- and beta-subunit polypeptides in rat brain. *J. Neurosci.* **15**, 5360–5371 (1995).
25. J. Du, J. H. Tao-Cheng, P. Zerfas, C. J. McBain, The K+ channel, Kv2.1, is apposed to astrocytic processes and is associated with inhibitory postsynaptic membranes in hippocampal and cortical principal neurons and inhibitory interneurons. *Neuroscience* **84**, 37–48 (1998).
26. J. S. Trimmer, Immunological identification and characterization of a delayed rectifier K+ channel polypeptide in rat brain. *Proc. Natl. Acad. Sci. U.S.A.* **88**, 10764–10768 (1991).
27. P. M. Hwang, M. Fotuhi, D. S. Bredt, A. M. Cunningham, S. H. Snyder, Contrasting immunohistochemical localizations in rat brain of two novel K+ channels of the Shab subfamily. *J. Neurosci.* **13**, 1569–1576 (1993).
28. H. I. Bishop *et al.*, Distinct cell- and layer-specific expression patterns and independent regulation of Kv2 channel subtypes in cortical pyramidal neurons. *J. Neurosci.* **35**, 14922–14942 (2015).
29. D. R. Hochbaum *et al.*, All-optical electrophysiology in mammalian neurons using engineered microbial rhodopsins. *Nat. Methods* **11**, 825–833 (2014).
30. I. H. Cho, L. C. Panzera, M. Chin, M. B. Hoppa, Sodium channel β2 subunits prevent action potential propagation failures at axonal branch points. *J. Neurosci.* **37**, 9519–9533 (2017).
31. D. E. Antonucci, S. T. Lim, S. Vassanelli, J. S. Trimmer, Dynamic localization and clustering of dendritic Kv2.1 voltage-dependent potassium channels in developing hippocampal neurons. *Neuroscience* **108**, 69–81 (2001).
32. P. D. Sarmiere, C. M. Weigle, M. M. Tamkun, The Kv2.1 K+ channel targets to the axon initial segment of hippocampal and cortical neurons in culture and in situ. *BMC Neurosci.* **9**, 112 (2008).
33. H. Misonou, D. P. Mohapatra, M. Menegola, J. S. Trimmer, Calcium- and metabolic state-dependent modulation of the voltage-dependent Kv2.1 channel regulates neuronal excitability in response to ischemia. *J. Neurosci.* **25**, 11184–11193 (2005).
34. B. C. Campbell *et al.*, mGreenLantern: A bright monomeric fluorescent protein with rapid expression and cell filling properties for neuronal imaging. *Proc. Natl. Acad. Sci. U.S.A.* **117**, 30710–30721 (2020).
35. R. H. Scannevin, H. Murakoshi, K. J. Rhodes, J. S. Trimmer, Identification of a cytoplasmic domain important in the polarized expression and clustering of the Kv2.1 K+ channel. *J. Cell Biol.* **135**, 1619–1632 (1996).
36. K. M. O'Connell, A. S. Rolig, J. D. Whitesell, M. M. Tamkun, Kv2.1 potassium channels are retained within dynamic cell surface microdomains that are defined by a perimeter fence. *J. Neurosci.* **26**, 9609–9618 (2006).
37. M. Kirmiz, N. C. Vierra, S. Palacio, J. S. Trimmer, Identification of VAPA and VAPB as Kv2 channel-interacting proteins defining endoplasmic reticulum-plasma membrane junctions in mammalian brain neurons. *J. Neurosci.* **38**, 7562–7584 (2018).
38. J. S. Trimmer, Expression of Kv2.1 delayed rectifier K+ channel isoforms in the developing rat brain. *FEBS Lett.* **324**, 205–210 (1993).
39. J. Suzuki *et al.*, Imaging intraorganellar Ca2+ at subcellular resolution using CEPIA. *Nat. Commun.* **5**, 4153 (2014).
40. S. T. Lim, D. E. Antonucci, R. H. Scannevin, J. S. Trimmer, A novel targeting signal for proximal clustering of the Kv2.1 K+ channel in hippocampal neurons. *Neuron* **25**, 385–397 (2000).
41. Y. Wu *et al.*, Contacts between the endoplasmic reticulum and other membranes in neurons. *Proc. Natl. Acad. Sci. U.S.A.* **114**, E4859–E4867 (2017).
42. J. Kuja-Panula, M. Kiiltomäki, T. Yamashiro, A. Rouhiainen, H. Rauvala, AMIGO, a transmembrane protein implicated in axon tract development, defines a novel protein family with leucine-rich repeats. *J. Cell Biol.* **160**, 963–973 (2003).
43. M. A. Peltola, J. Kuja-Panula, S. E. Lauri, T. Taira, H. Rauvala, AMIGO is an auxiliary subunit of the Kv2.1 potassium channel. *EMBO Rep.* **12**, 1293–1299 (2011).
44. M. B. Hoppa, G. Gouzer, M. Armbruster, T. A. Ryan, Control and plasticity of the presynaptic action potential waveform at small CNS nerve terminals. *Neuron* **84**, 778–789 (2014).
45. H. Xu *et al.*, Attenuation of the slow component of delayed rectification, action potential prolongation, and triggered activity in mice expressing a dominant-negative Kv2 alpha subunit. *Circ. Res.* **85**, 623–633 (1999).
46. S. M. Voglmaier *et al.*, Distinct endocytic pathways control the rate and extent of synaptic vesicle protein recycling. *Neuron* **51**, 71–84 (2006).
47. P. Ariel, M. B. Hoppa, T. A. Ryan, Intrinsic variability in Pv, RRP size, Ca(2+) channel repertoire, and presynaptic potentiation in individual synaptic boutons. *Front. Synaptic Neurosci.* **4**, 9 (2013).
48. G. Miesenböck, D. A. De Angelis, J. E. Rothman, Visualizing secretion and synaptic transmission with pH-sensitive green fluorescent proteins. *Nature* **394**, 192–195 (1998).
49. S. Sankaranarayanan, D. De Angelis, J. E. Rothman, T. A. Ryan, The use of pHluorins for optical measurements of presynaptic activity. *Biophys. J.* **79**, 2199–2208 (2000).
50. J. Herrington *et al.*, Blockers of the delayed-rectifier potassium current in pancreatic beta-cells enhance glucose-dependent insulin secretion. *Diabetes* **55**, 1034–1042 (2006).
51. H. Li *et al.*, Concurrent imaging of synaptic vesicle recycling and calcium dynamics. *Front. Mol. Neurosci.* **4**, 34 (2011).
52. T. W. Chen *et al.*, Ultrasensitive fluorescent proteins for imaging neuronal activity. *Nature* **499**, 295–300 (2013).
53. A. Penna *et al.*, The CRAC channel consists of a tetramer formed by Stim-induced dimerization of Orai dimers. *Nature* **456**, 116–120 (2008).
54. C. Y. Park, A. Shcheglovitov, R. Dolmetsch, The CRAC channel activator STIM1 binds and inhibits L-type voltage-gated calcium channels. *Science* **330**, 101–105 (2010).
55. S. B. Baver, K. M. O'Connell, The C-terminus of neuronal Kv2.1 channels is required for channel localization and targeting but not for NMDA-receptor-mediated regulation of channel function. *Neuroscience* **217**, 56–66 (2012).
56. N. J. Emptage, C. A. Reid, A. Fine, Calcium stores in hippocampal synaptic boutons mediate short-term plasticity, store-operated Ca2+ entry, and spontaneous transmitter release. *Neuron* **29**, 197–208 (2001).
57. Y. Liang, L. L. Yuan, D. Johnston, R. Gray, Calcium signaling at single mossy fiber presynaptic terminals in the rat hippocampus. *J. Neurophysiol.* **87**, 1132–1137 (2002).
58. F. W. Lindhout *et al.*, VAP-SCRN1 interaction regulates dynamic endoplasmic reticulum remodeling and presynaptic function. *EMBO J.* **38**, e101345 (2019).
59. N. L. Chanaday *et al.*, Presynaptic store-operated Ca^{2+} entry drives excitatory spontaneous neurotransmission and augments endoplasmic reticulum stress. *Neuron* **109**, 1314–1332.e5 (2021).
60. P. J. Dittmer, A. R. Wild, M. L. Dell'Acqua, W. A. Sather, STIM1 Ca^{2+} sensor control of L-type Ca^{2+}-channel-dependent dendritic spine structural plasticity and nuclear signaling. *Cell Rep.* **19**, 321–334 (2017).
61. H. Misonou *et al.*, Bidirectional activity-dependent regulation of neuronal ion channel phosphorylation. *J. Neurosci.* **26**, 13505–13514 (2006).
62. H. Misonou, S. M. Thompson, X. Cai, Dynamic regulation of the Kv2.1 voltage-gated potassium channel during brain ischemia through neuroglial interaction. *J. Neurosci.* **28**, 8529–8538 (2008).
63. H. Misonou *et al.*, Regulation of ion channel localization and phosphorylation by neuronal activity. *Nat. Neurosci.* **7**, 711–718 (2004).
64. T. Tanabe, K. G. Beam, J. A. Powell, S. Numa, Restoration of excitation-contraction coupling and slow calcium current in dysgenic muscle by dihydropyridine receptor complementary DNA. *Nature* **336**, 134–139 (1988).
65. T. Tanabe, K. G. Beam, B. A. Adams, T. Niidome, S. Numa, Regions of the skeletal muscle dihydropyridine receptor critical for excitation-contraction coupling. *Nature* **346**, 567–569 (1990).
66. G. Ashrafi, J. de Juan-Sanz, R. J. Farrell, T. A. Ryan, Molecular tuning of the axonal mitochondrial Ca^{2+} uniporter ensures metabolic flexibility of neurotransmission. *Neuron* **105**, 678–687.e5 (2020).
67. C. O. Wong *et al.*, A TRPV channel in Drosophila motor neurons regulates presynaptic resting Ca2+ levels, synapse growth, and synaptic transmission. *Neuron* **84**, 764–777 (2014).
68. E. E. Maverick, A. N. Leek, M. M. Tamkun, Kv2 channel-AMIGO β-subunit assembly modulates both channel function and cell adhesion molecule surface trafficking. *J. Cell Sci.* **134**, jcs256339 (2021).
69. W. P. Bartlett, G. A. Banker, An electron microscopic study of the development of axons and dendrites by hippocampal neurons in culture. I. Cells which develop without intercellular contacts. *J. Neurosci.* **4**, 1944–1953 (1984).
70. G. J. Brewer, J. R. Torricelli, E. K. Evege, P. J. Price, Optimized survival of hippocampal neurons in B27-supplemented Neurobasal, a new serum-free medium combination. *J. Neurosci. Res.* **35**, 567–576 (1993).